Electronic Supplementary Information†

Custom design of solid-solid phase change material with ultra-high thermal stability for battery thermal management

Changren Xiao, Guoqing Zhang, Zhenghui Li, Xiaoqing Yang*

School of Materials and Energy, Guangdong University of Technology, Guangzhou 510006, PR China

Experimental Section

Fast-paced synthesis of SSPoPCM/EG-6%-10min: 182.5 g octadecyl acrylate (OA), 3.5 g 1, 6-hexanediol diacrylate (HDDA), and 1.5 g benzoyl peroxide (BPO) were first added into a stainless-steel container successively, and then heated in a 50℃ oil bath to form a clear solution. After that, 12 g EG (mass fraction of 6wt%), as the thermal conductive filler, was added into the solution with mechanical stirring until a homogeneous dispersive mixture was obtained. The homogeneous reactants prior to cross-linking were casted to a steel mold on the heating stage and the temperature of the stage was subsequently raised to 90℃ for 10 minutes, during which a video was shot (Video S1). The thermo-physical properties of the obtained SSPoPCM/EG-6%-10min are shown in Table S2.

Synthetic process of polymer phase change materials (PoPCM) with different dosages and types of crosslinkers: Different crosslinkers of divinyl benzene (DVB), HDDA or diallyl terephthalate (DATP), BPO and monomer of OA were added into a three-neck flask at 50°C under magnetic stirring to obtain a clear solution. The solution was then heated to 90°C for 1 h to initiate and conduct the polymerization reaction. A series of PoPCMs with different molar ratios (crosslinker/monomer) of 1:20, 1:40 and 1:60 were

* Corresponding author.
E-mail address: yangxiaoqing@gdut.edu.cn (X. Yang)

thus prepared. The specimen polymerized without crosslinkers was labelled as POA, and specimen polymerized with different crosslinkers at the optimal molar ratio, which exhibited the highest latent heat (phase change enthalpy, ΔH_m), was denoted as PoPCM-DVB, PoPCM-HDDA and PoPCM-DATP, respectively. Their corresponding DSC curves are shown in Figure S4.

Preparation process of traditional PA/LDPE/EG ternary solid-liquid CPCM (SLPCM): 538 g PA was melted in an 85°C-oil bath pot for 1 h. 50.5 g EG (6wt%) was added slowly into a stainless-steel vessel under continuous mechanical stirring. Then 251.5 g low-density polyethylene (LDPE) was added into the mixture and the temperature of the oil bath was raised to 145°C. After that, the molten composite was poured into the mold with various dimensions and then moved into an oven of 130°C for 0.5 h to eliminate the air bubbles existed. Subsequently, the resultant composite was cooled to room temperature naturally. This PA-based CPCM was denoted as SLPCM/EG-6% (Figure S3) [1] .

Experiment setup of thermal resistance tests: The diagram and digital graph of the experimental apparatus are shown in Figure S10 and S11 based on our previous reports[2]. A ceramic plate heater simulating the heat source, was attached to the surface of the aluminum substrate. The input powers of 3 and 6 W were supplied respectively from an independently controlled AC power unit. The whole aluminum substrate, except the upper surface, was insulated with thermal insulation material of melamine sponge with a low thermal conductivity, to minimize the thermal loss. To investigate the thermal resistance of different PCMs, the upper surface of the Al substrate was covered with SLPCM/EG-6% or SSPoPCM/EG-6% board, as physically displayed in Figure S10. The thermal conductive silicon grease was carefully applied to reduce the thermal contact resistance between the aluminum substrate and the PCM boards. Omega J-type thermocouples were placed to the central position of two opposite surfaces of the PCM board and the temperature was recorded by a Fluke data logger.

Figure

Figure S1. Three basic requirements for PCMs feasible in BTM application

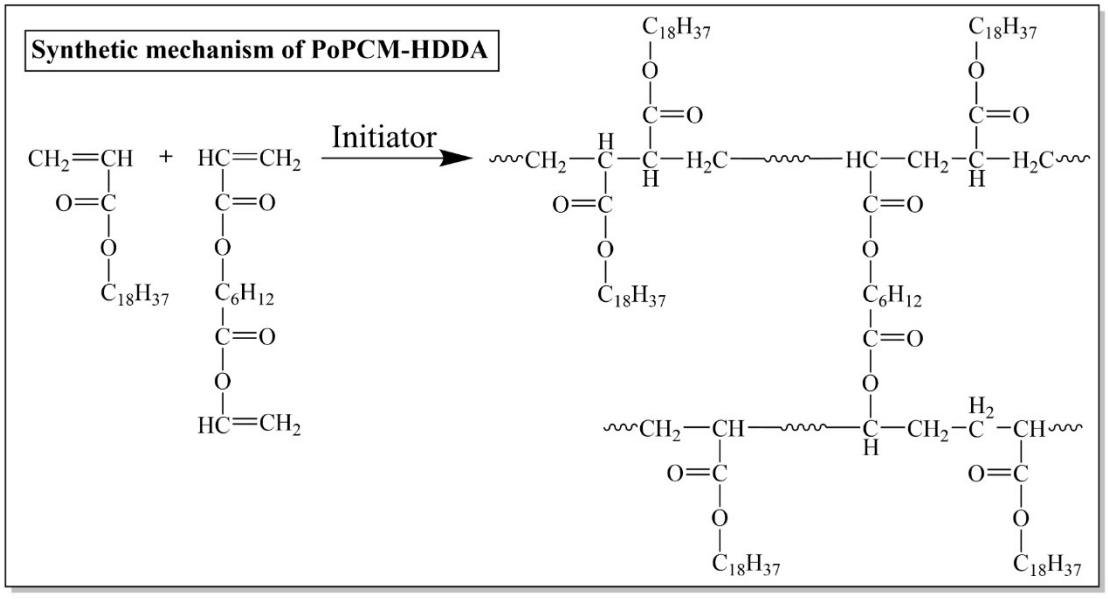

Figure S2. Synthetic mechanism of PoPCM using HDDA as the crosslinker

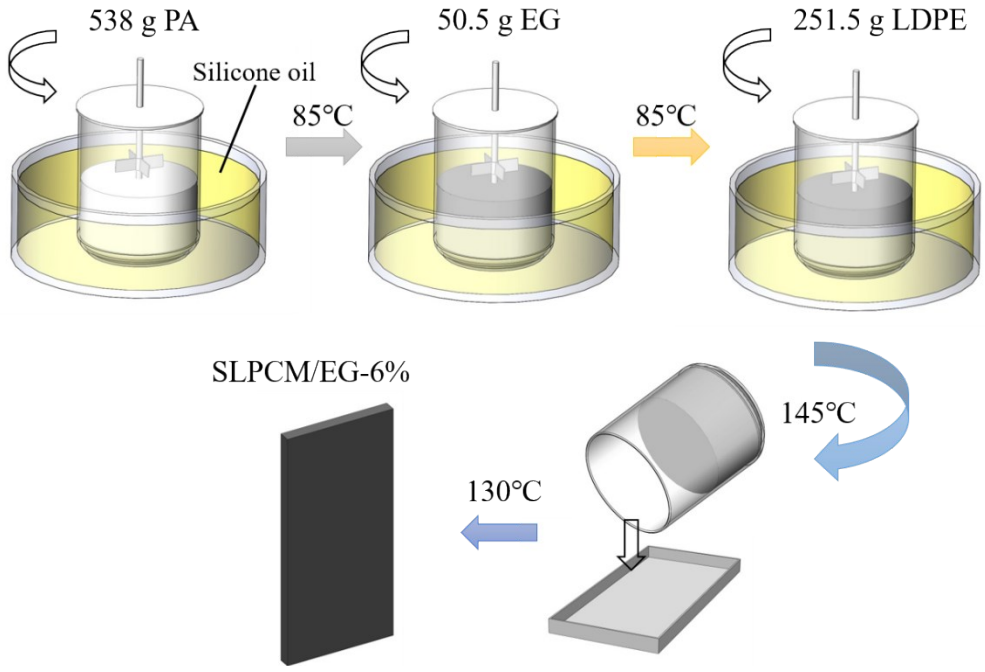

Figure S3. Preparation procedures of SLPCM/EG-6%

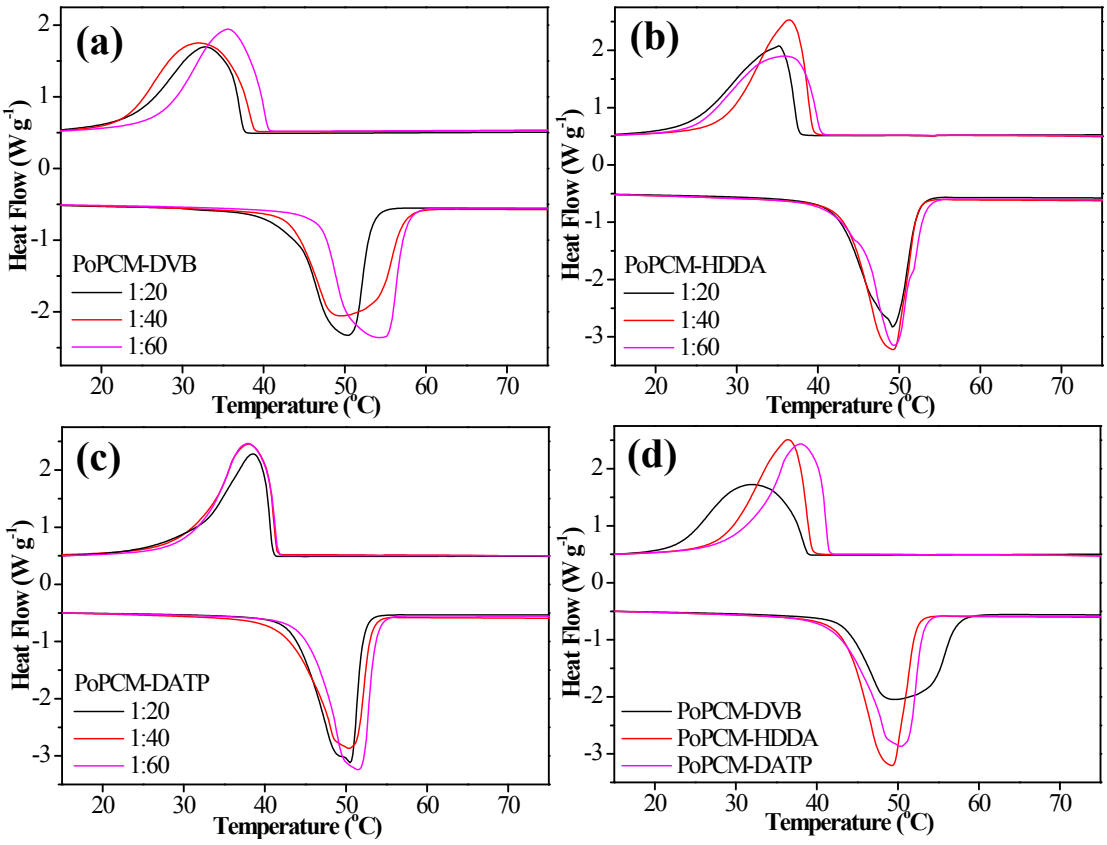

Figure S4. DSC curves of the PoPCMs synthesized using various dosages and types of crosslinkers.

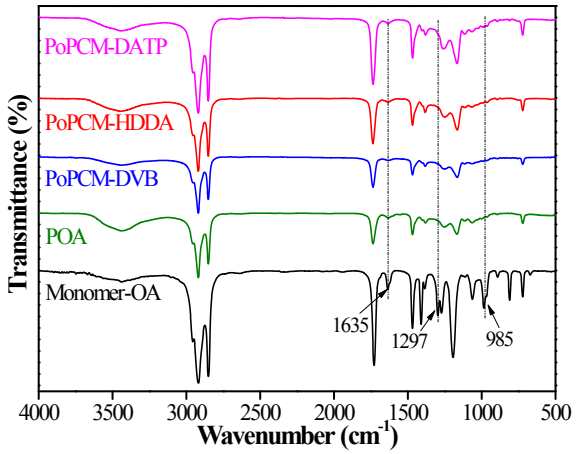

Figure S5. FTIR spectra of OA, POA, PoPCM-DVB, PoPCM-HDDA and PoPCM-DATP

As seen from the FTIR spectra from Figure S5, in all samples, the peaks at 2956, 2925 and 2855 cm^{-1} are ascribed to the alkyl C-H stretching vibrations of the methyl and methylene groups. The peak at 1729 cm^{-1} can be assigned to the C=O stretching vibration of the ester group, and the C-O stretching vibration of the ester group triggers intensive absorption peaks at 1269 and 1191 cm^{-1}. The spectra also demenstrate an absorption peak at 721 cm^{-1} corresponding to the in-plane rocking vibration of methylene derived from the stearyl (C18) groups. It is noted that after polymerization, the characteristic vibration peaks of C=C at 1635 cm^{-1}, vinyl C-H at 1297 cm^{-1} and 985 cm^{-1} are absent, which reflects the successful synthesis of the 3D cross-linking structure with C18 side chains[3] .

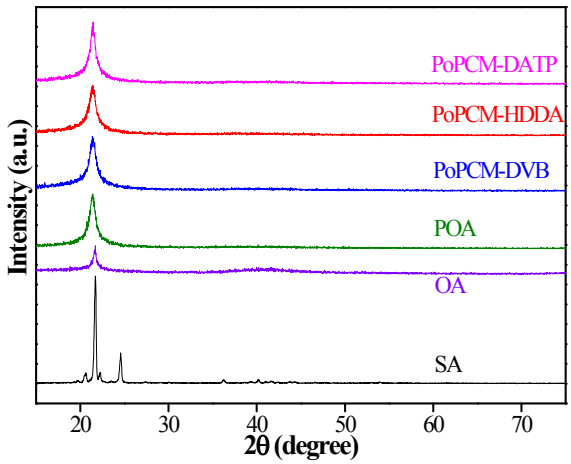

Figure S6. XRD patterns of SA (stearyl alcohol), OA, POA, PoPCM-DVB, PoPCM-HDDA and PoPCM-DATP

In the XRD patterns (Figure S6), all samples exhibit a similar intense diffraction peak at 2θ of around 21.4°, indicative of a good crystalline derived from the C18 group.

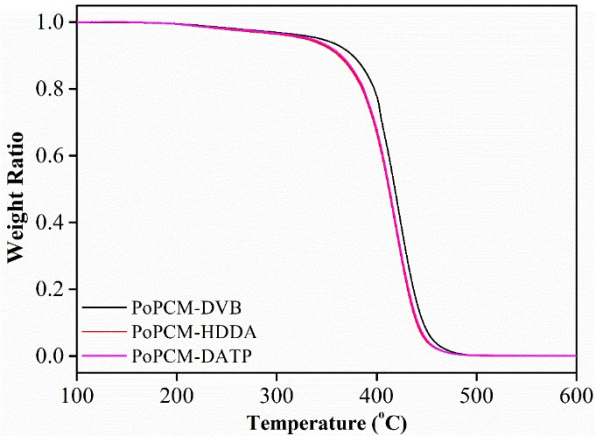

Figure S7. TG curves of PoPCM-DVB, PoPCM-HDDA, PoPCM-DATP in nitrogen atmosphere

As seen from Figure S7, large mass loss of all samples occurs after 400°C in nitrogen atmosphere, further confirming the ultra-high thermal stability of our conceived PoPCMs.

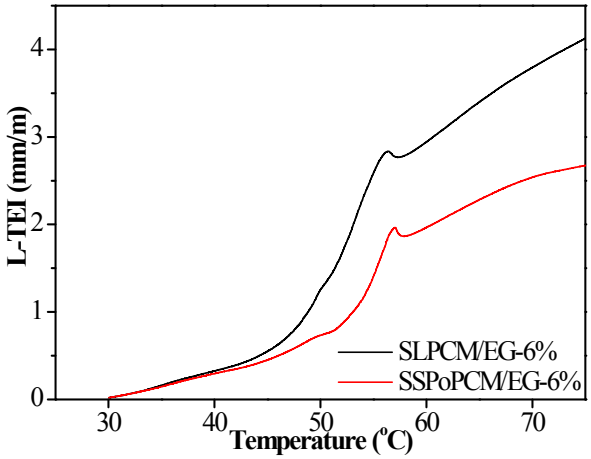

Figure S8. Linear thermal expansion increment (L-TEI) curves of SLPCM/EG-6% and SSPoPCM/EG-6%

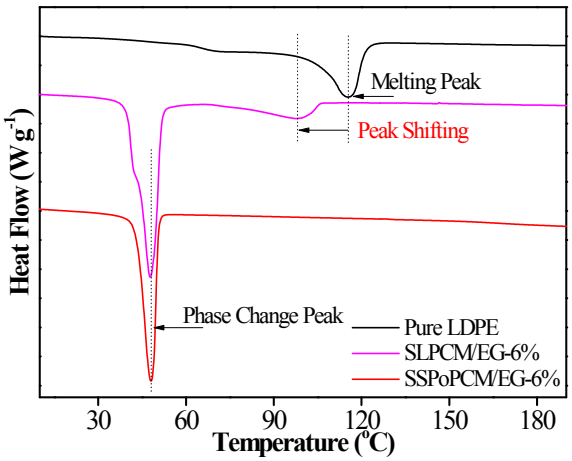

Figure S9. DSC curves of pure LDPE, SLPCM/EG-6% and SSPoPCM/EG-6%

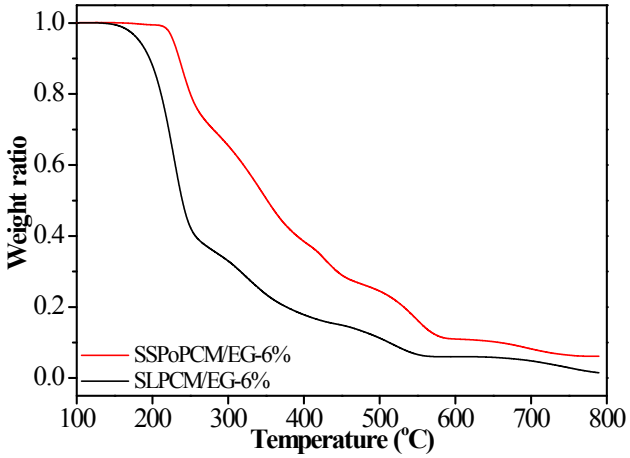

Figure S10. TG curves of SLPCM/EG-6% and SSPoPCM/EG-6%

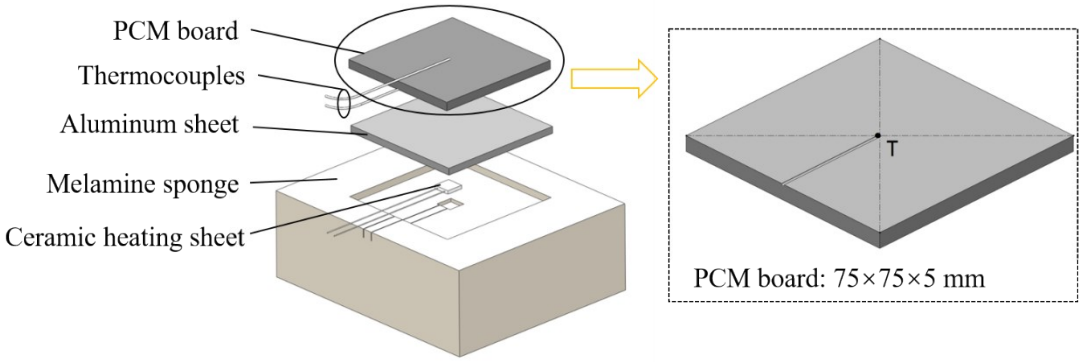

Figure S11. Experimental setup diagram of thermal resistance tests

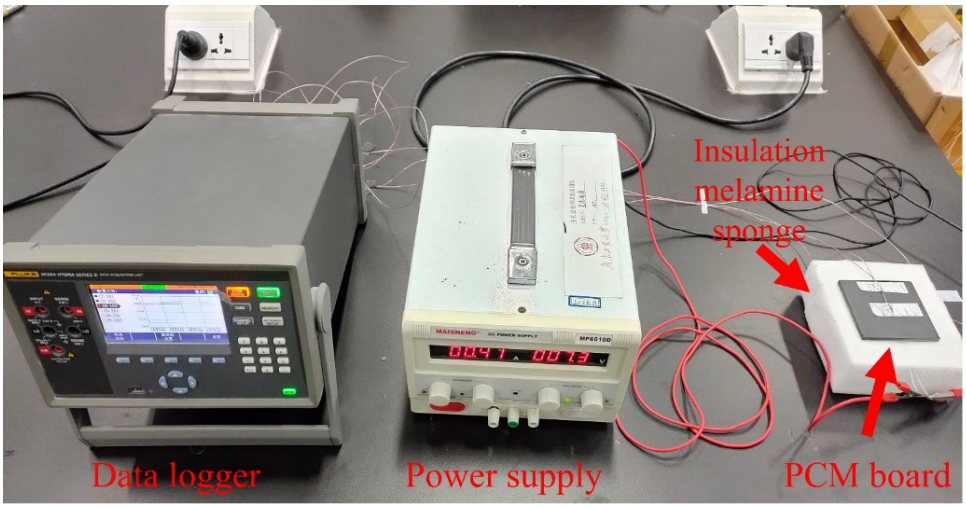

Figure S12. Digital graph of the experimental setup of thermal resistance tests

Table

Table S1. Thermal conductivity of CPCMs with different kinds and contents of thermal conductive fillers

CPCM composition	Thermal conductive ingredient (mass content)	Thermal conductivity ($W\ m^{-1}\ K^{-1}$)	References
PA/LDPE/EG	EG (7wt%)	1.13	[4]
PA/LDPE/EG	EG (7wt%)	1.38	[1]
PA/ER/EG/SiC	EG (3wt%)/SiC (5wt%)	1.31	[5]
PA/ER/EG/AlN	EG (3wt%)/AlN (5wt%)	1.13	[6]
PA/ER/EG	EG (6wt%)	0.63	[7]
PA/GO	GO (55wt%)	1.32	[8]
PA/OBC/EG	EG (3wt%)	1.18	[9]
PA/EG	EG (6wt%)	1.42	[10]

Abbreviations: CPCM (composite phase change material); PA (paraffin); LDPE (low density polyethylene); EG (expanded graphite); ER (epoxy resin); SiC (silicon carbide); AlN (Aluminum nitride), GO (graphene oxide); OBC (olefin block copolymer)

Table S2. Thermo-physical properties of SSPoPCM/EG-6%-10min

T_{mp} (°C)	ΔH_m ($J\ g^{-1}$)	Thermal conductivity ($W\ m^{-1}\ K^{-1}$)
46.8	92.4	2.29

T_{mp}: melting peak temperature; ΔH_m: phase change enthalpy

Table S3. Basic parameters of the pouch cells

Parameters	Value
Quality (g)	299.0±5.0
Rated capacity (Ah)	16
Rated voltage (V)	3.7
Open-circuit voltage (V)	4.2

Table S4. Parameters of the charge-discharge tests with different discharge rates

Process	Time (min)	Current	Voltage
Constant current charge	-	8 A (0.5 C)	Cut-off voltage of 21 V
Constant voltage charge	-	Cut-off current of 0.2 A	21 V
Rest	240	-	-
Constant current discharge	-	16-80 A (1-5 C)	Cut-off voltage of 15 V
Rest	120	-	-

Table S5. Parameters of cyclic charge-discharge tests

Process	Time (min)	Current	Voltage
Constant current charge	-	8 A (0.5 C)	Cut-off voltage of 21 V
Constant voltage charge	-	Cut-off current of 0.2 A	21 V
Rest	30	-	-
Constant current discharge	-	80 A (5 C)	Cut-off voltage of 15 V
Rest	30	-	-

Table S6. DSC data of different PoPCMs with various dosages and types of crosslinkers

DVB/OA	T_{mp} (°C)	ΔH_m (J g^{-1})	HDDA/OA	T_{mp} (°C)	ΔH_m (J g^{-1})	DATP/OA	T_{mp} (°C)	ΔH_m (J g^{-1})
1:20	49.9	79.5	1:20	48.7	91.6	1:20	50.1	89.7
1:40	49.1	92.5	1:40	48.9	98.8	1:40	49.9	98.6
1:60	53.8	89.4	1:60	48.8	92.3	1:60	50.1	91.8

T_{mp}: phase change peak temperature

Table S7. ΔH_m variation of SLPCM/EG-6% and SSPoPCM/EG-6% before and after 100 endothermic and exothermic cycles

Samples	ΔH_m(J g^{-1})				
	Before Cycling	After cycling			Decline rate (%)
		Upper Surface	Lower Surface	Mean value	
SLPCM/EG-6%	117.5	98.7	103.5	101.1	14.0
SSPoPCM/EG-6%	91.3	90.5	90.6	90.6	-

Table S8. Thermal steady temperature and calculated thermal resistance of SLPCM/EG-6% and SSPoPCM/EG-6% boards at different power levels

Power levels	Samples	T_{PCM-l} (°C)	T_{PCM-u} (°C)	T_{air} (°C)	R_{PCM} (°C W^{-1})	$R_{PCM-Air}$ (°C W^{-1})	R_{total} (°C W^{-1})
3 W	SLPCM/EG-6%	52.1	47.4	22.0	1.6	8.5	10.1
	SSPoPCM/EG-6%	49.2	46.7	22.2	0.8	8.2	9.0
6 W	SLPCM/EG-6%	77.6	66.5	21.8	1.9	7.5	9.4
	SSPoPCM/EG-6%	73.7	68.5	22.3	0.9	7.7	8.6

Table S9. T_{max} and ΔT_{max} of the SLPCM and SSPoPCM modules in odd-numbered cycles

Cycle	SLPCM module		SSPoPCM module	
	T_{max}	ΔT_{max}	T_{max}	ΔT_{max}
1	46.6	4.3	44.8	3.2
3	46.9	4.1	45.4	3.0
5	46.9	4.1	45.1	3.1
7	46.8	4.1	45.1	3.0
9	46.9	4.1	45.3	3.0
11	46.7	4.1	45.3	3.1

13	46.9	4.1	45.0	3.0
15	46.8	4.0	45.1	3.1
17	46.9	4.1	45.2	3.1
19	46.7	4.0	45.3	3.0

Reference

1. Y. F. Lv, X. Q. Yang, X. X. Li, G. Q. Zhang, Z. Y. Wang and C. Z. Yang, *Appl. Energy*, 2016, **178**, 376-382.
2. W. Wu, G. Zhang, X. Ke, X. Yang, Z. Wang and C. Liu, *Energy Convers. Manage.*, 2015, **101**, 278-284.
3. Y. Mao, J. Gong, M. Zhu and H. Ito, *Polym.*, 2018, **150**, 267-274.
4. Y. F. Lv, W. F. Situ, X. Q. Yang, G. Q. Zhang and Z. Y. Wang, *Energy Convers. Manage.*, 2018, **163**, 250-259.
5. W. Yuan, X. Yang, G. Zhang and X. Li, *Appl. Therm. Eng.*, 2018, **144**, 551-557.
6. J. Y. Zhang, X. X. Li, G. Q. Zhang, Y. Z. Wang, J. W. Guo, Y. Wang, Q. Q. Huang, C. R. Xiao and Z. D. Zhong, *Energy Convers. Manage.*, 2019, **245**, 112319.
7. J. He, X. Yang and G. Zhang, *Appl. Therm. Eng.*, 2019, **148**, 984-991.
8. M. Mehrali, S. T. Latibari, M. Mehrali, H. S. C. Metselaar and M. Silakhori, *Energy Convers. Manage.*, 2013, **67**, 275-282.
9. Y.-H. Huang, W.-L. Cheng and R. Zhao, *Energy Convers. Manage.*, 2019, **182**, 9-20.
10. F. He, X. Li, G. Zhang, G. Zhong and J. He, *Int. J. Energy Res.*, 2018, **42**, 3279-3288.